Supporting Information

ZIF-67-derived Co-NC@CoP-NC nanopolyhedrals as efficient bifunctional electrocatalysts for the oxygen reaction and evolution reaction

Xingyue Li,[a, +] Qianqian Jiang,[b] Shuo Dou,[a] Libo Deng,[b] Jia Huo,[a,*] and Shuangyin Wang [a,*]

Section 1. Materials and Instrumentation

All chemicals are from commercial and used without further purification: Cobaltousnitrate hexahydrate ($Co(NO_3)_2·6H_2O$,98.5%, Sinopharm Chemical Reagent Co., Ltd.), 2-methylimidazole (99.0%, Aladdin), NaH_2PO_2 (Shanghai Titanchem Co.,Ltd), methanol (99.5%, Sinopharm Chemical Reagent Co., Ltd.), ethanol (99.7%, Shanghai Titan Scientific Co.,Ltd), and de-ionized water with the specific resistance of 18.25 MΩ·cm (obtained by reversed osmosis followed by ion-exchange and filtration (Cleaned Water Treatment Co., Ltd., Hefei)).

Experimental Section

Synthesis of ZIF-67 crystals: $Co(NO_3)_2.6H_2O$ (1.455 g) and 2-methylinidazole (1.642 g) were dissolved in the binary mixture of 40 ml methanol (MeOH) and 40 ml ethanol (EtOH) respectively. The above two solutions were sonicated for 5 min respectively and then mixed vigorously for 30 s. Then the resulting solution was stood at room temperature for 24 h. The resulting purple precipitates were collected by centrifugation, washed with ethanol several times, and vacuum-dried at 60 °C.

Synthesis of Co@NC: The obtained ZIF-67 (200 mg) was put in a porcelain boat, which was put in the middle of a quartz tube in a furnace charged with nitrogen gas. The temperature inside the furnace was gradually increased from room temperature to the target temperature (600,700, 800 and 900 °C) for 3 h at a heating rate of 5 $°C·min^{-1}$ to obtain Co@NC-x, wherein "x" represents the carbonization temperature.

Preparation of Co-NC@CoP-NC: Co@NC-x and NaH_2PO_2 were put into two separate porcelain boats with NaH_2PO_2 at the upstream side of the furnace. Subsequently, the sample was heated at 350 °C for 2h in a static Ar atmosphere, and then naturally cooled to ambient temperature under Ar.

Samples with different ratio of precursor powders and NaH_2PO_2 also were obtained by phosphidation of Co-N-C@CoP-N-C with different amount of NaH_2PO_2. CoP@NC was synthesized by heating NaH_2PO_2 and ZIF-67 together at 700°C.

Characterizations:

The Raman spectra were collected on a Raman spectrometer (Labram-010) using 632nm laser. The morphology of all sample were determined by scanning electron microscopy (SEM, Hitachi, S-4800) and transmission electron microscopy (TEM, Tecnai g2 F20). The crystal structures of the samples were characterized using powder X-ray diffraction (XRD, Bruker D8 Advance diffract meter, Cu Kα1). The nitrogen adsorption-desorption isotherms were measured at 77 K with a Quantachrom NOVA 1000e system. X-ray photoelectron spectroscopy (XPS) analysis was performed on an ESCALAB 250Xi X-ray photoelectron spectrometer using Mg as the excitation source. The thermogravimetric analysis (TGA) was carried out on a TA instrument with a heating rate of 10 °C·min^{-1} in air.

Section 2. Catalytic Performance

All the electrochemical measurements were conducted in a typical three-electrode setup with an electrolyte solution of 0.1 M KOH, a working electrode, a Pt counter electrode, and a saturated calomel electrode (SCE) reference electrode. In all measurements, the SCE reference electrode was calibrated with respect to reversible hydrogen electrode (RHE). LSV measurements were conducted in 0.1 M KOH with scan rate of 5 mV·s^{-1}. All the potentials reported in our work were vs. the reversible hydrogen electrode (RHE). E (RHE) = E (SCE) + 0.059lgpH+0.244.

Preparation of working electrodes: Catalyst ink was prepared by dispersing 4 mg of catalyst into 1 mL of ethanol solvent containing 50 μL of 5 wt% Nafion through sonication for 90 min. Then 8.9 μL of the catalyst ink was loaded onto a glass-carbon electrode (GCE) of 4 mm in diameter (loading~ 0.283 mg·cm^{-2}).

Investigation of reaction mechanism of ORR process

To investigate the catalyst made on planner electrode, we obtained CV with different loadings on work electrode in Fig.S15a. The result indicated that the loading and current density were fitted well to a linear relationship (S15b), which shows that it was a thin film electrode.

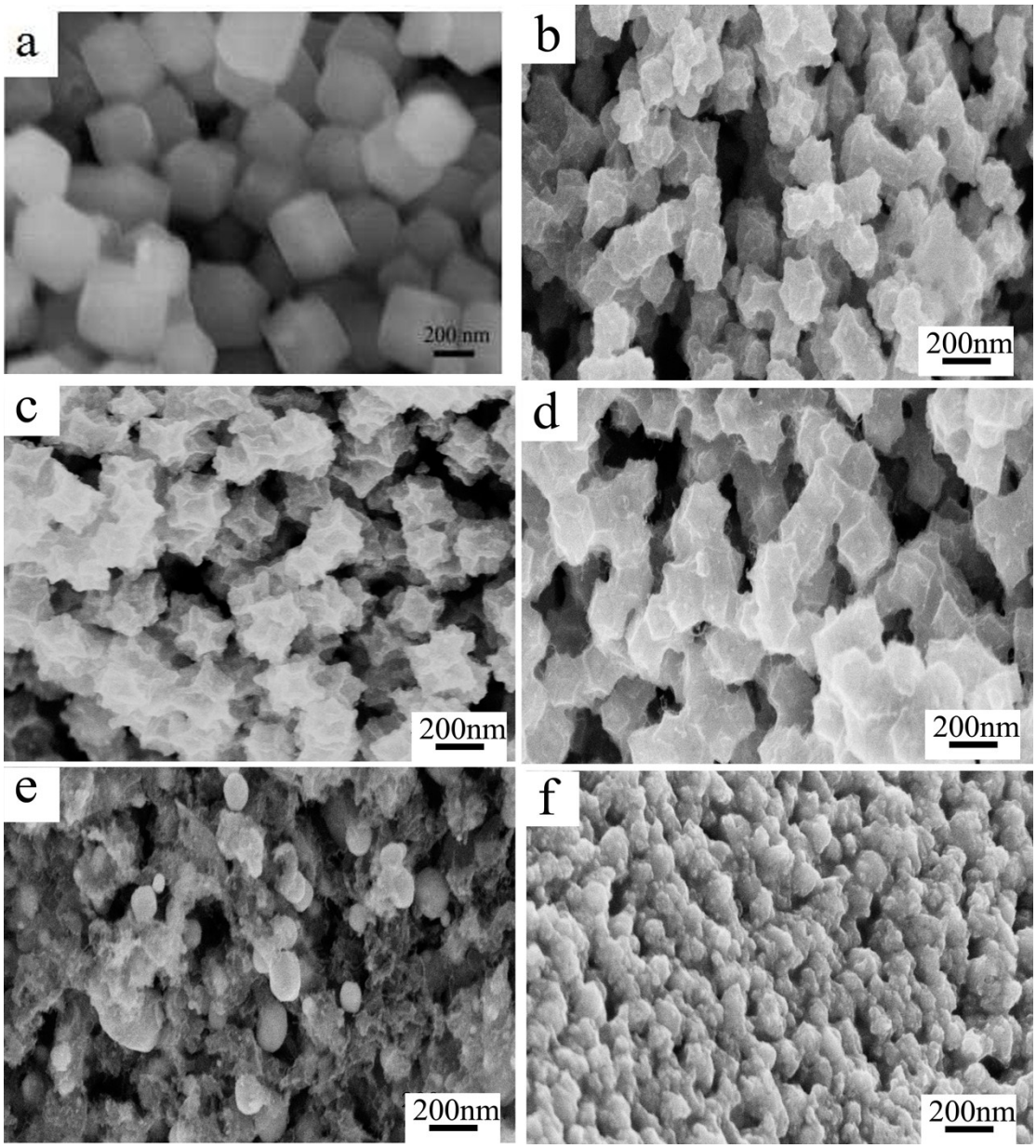

Fig. S1 (a) Typical SEM image of ZIF-67. SEM images of Co@NC-x (b) 600, (c) 700, (d) 800 and (e) 900 °C concave nanopolyhedrals. (f) Pure CoP@NC-700

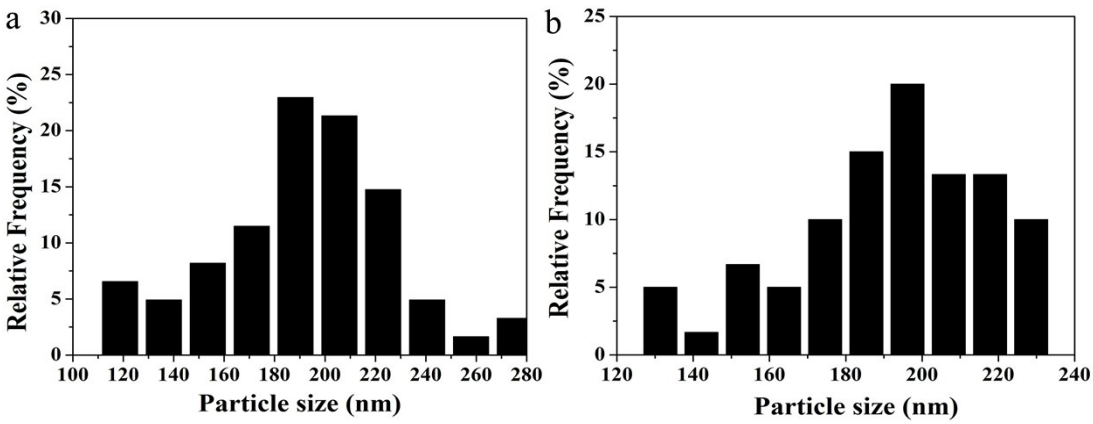

Fig. S2 The diameter distribution of (a) Co@NC and (b) Co-NC@CoP-NC.

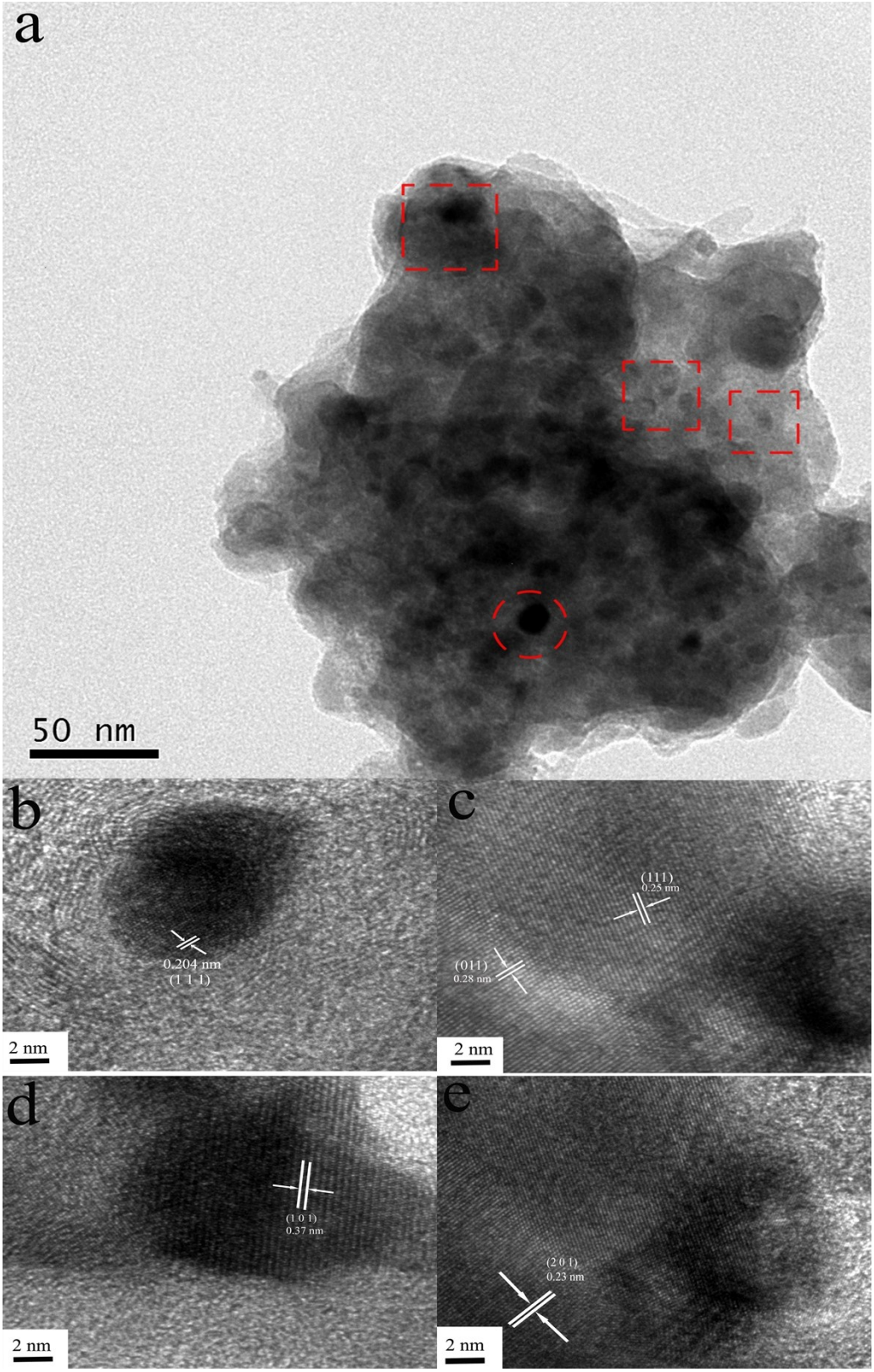

Fig. S3 (a) Low-magnification TEM image of Co-NC@CoP-NC. (b) HRTEM image of Co with the d spacing of (111) plane indicated. (c), (d), and (e) HRTEM images of CoP with the d spacing of (111), (011); (101) and (201) plane indicated, respectively. Square: the distribution of CoP. Circle: the distribution of Co.

Table S1 Energy dispersive X-ray (EDX) analyses of Co-NC@CoP-NC

element	wt %	at %
C K	30.07	49.74
N K	3.10	4.40
O K	22.86	28.39
P K	8.39	5.38
Co K	35.37	11.92
Al K	0.22	0.16
total	100	100

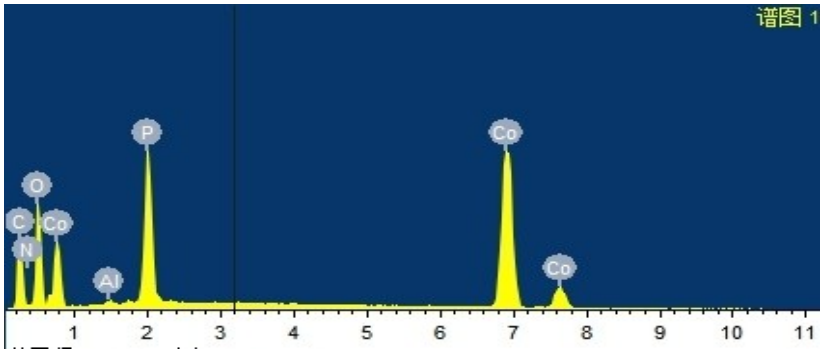

Fig. S4 The Energy dispersive X-ray (EDX) image of Co-NC@CoP-NC

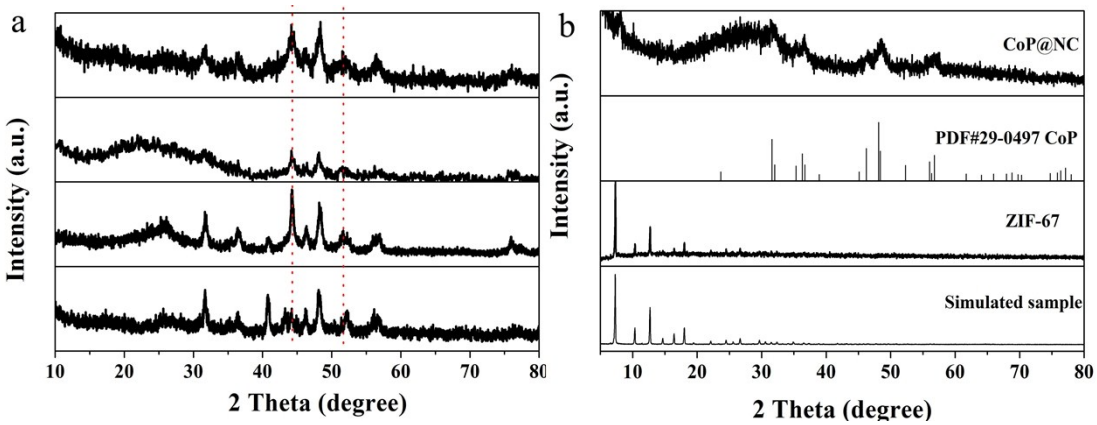

Fig. S5 XRD patterns of (a) Co-NC@CoP-NC –X. (X=600, 700, 800 and 900 °C, red line: XRD patterns of Co). (b) Pure ZIF-67 and ZIF-67.

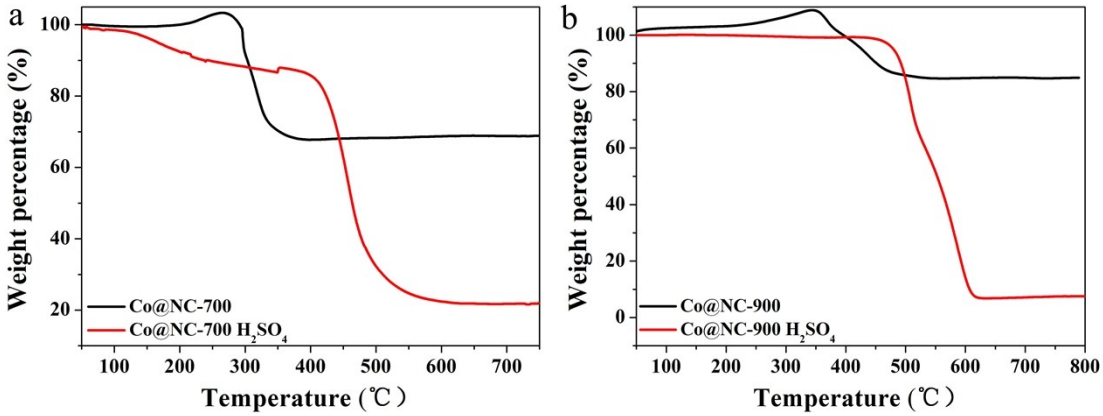

Fig.S6 The thermogravimetric analysis (TGA) curves of Co@NC-700 (a) and Co@NC-900 (b) before (black) and after (red) acid treatment 24h.

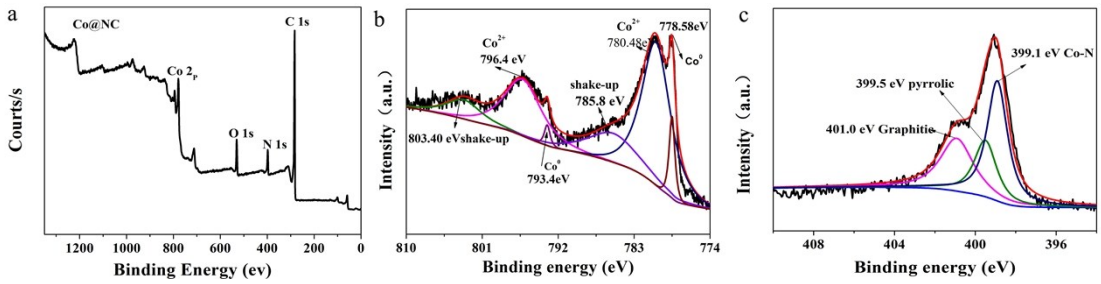

Fig. S7 (a) Survey XPS spectra of Co@NC. (b) Co 2p spectrum of Co@NC. (c) N1s spectrum of Co@NC

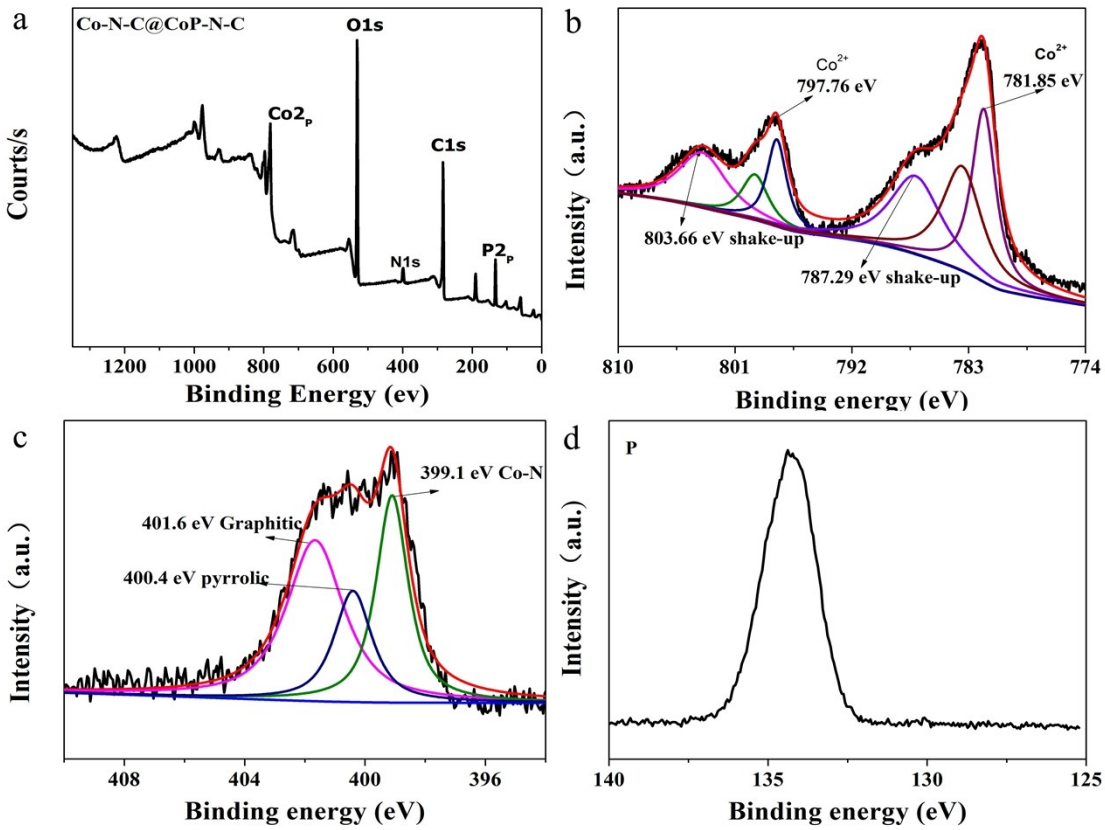

Fig. S8 (a) Survey XPS spectrum of Co-NC@CoP-NC. (b) Co 2p spectrum of Co-NC@CoP-

NC. (c) N1s spectrum of Co-NC@CoP-NC. (d) P spectrum of Co-NC@CoP-NC.

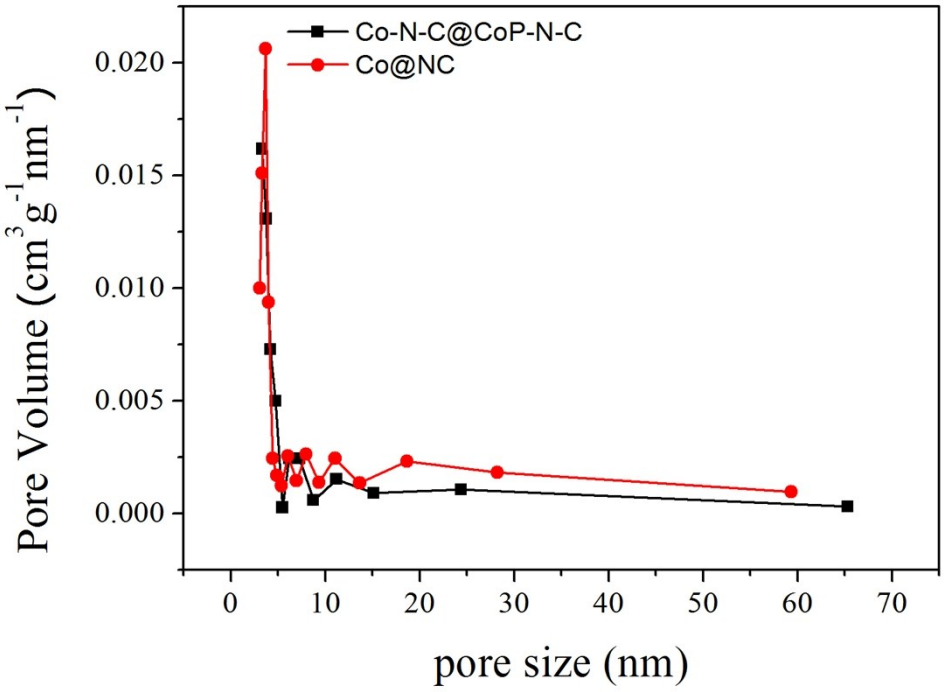

Fig.S9 Pore distribution profiles of Co-NC@CoP-NC and Co@NC.

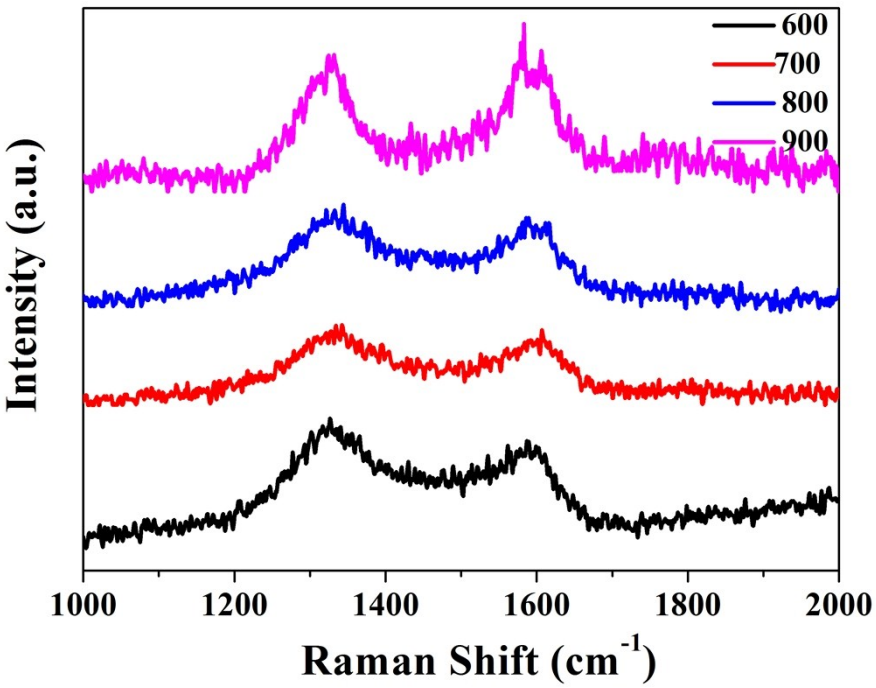

Fig. S10 The Raman spectra of Co-NC@CoP-NC-x (X=600,700,800,900 °C).

Table S2 The ratio of D and G peak for samples prepared with different pyrolysis temperature.

Co-NC@CoP-NC-600	I_D/I_G	1.53
Co-NC@CoP-NC-700	I_D/I_G	1.10
Co-NC@CoP-NC-800	I_D/I_G	1.06
Co-NC@CoP-NC-900	I_D/I_G	0.97

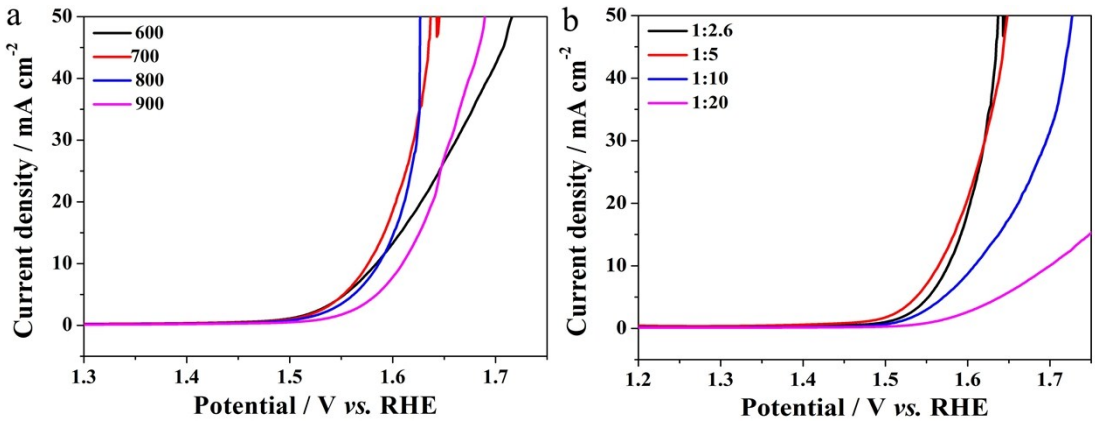

Fig. S11 (a) The polarization curves of OER on Co-NC@CoP-NC –X. (X=600, 700, 800 and 900 °C). (b) The polarization curves of OER on Co-NC@CoP-NC-700 prepared with different ratio between precursor powders and NaH_2PO_2.

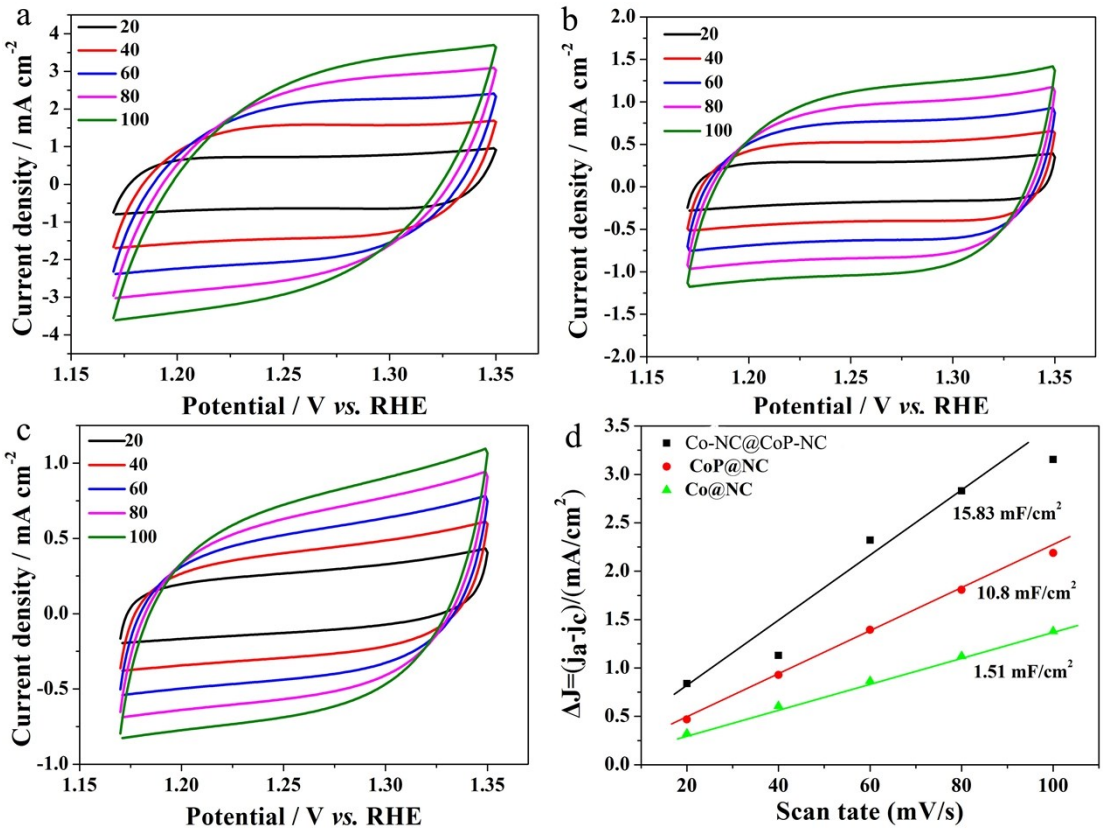

Fig. S12 Cyclic voltammetry curves of (a) Co-NC@CoP-NC, (b) CoP@NC and (c) Co@NC. (d) The capacitive current measured at 1.26 V vs RHE was plotted as a function of scan rate.

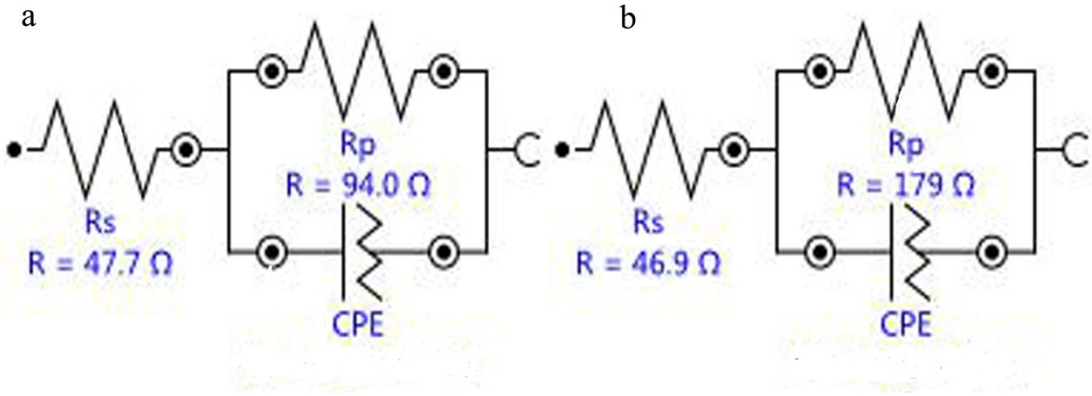

Fig. S13 Electrochemical impedance spectroscopy (EIS) fitting results for Co-NC@CoP-NC and Co@NC were recorded at 1.54 V vs. RHE. The equivalent circuits consisting of an electrolyte resistance (Rs), a charge-transfer resistance (Rp) and a constant-phase element (CPE) for Co-NC@CoP-NC (a) and Co@NC (b).

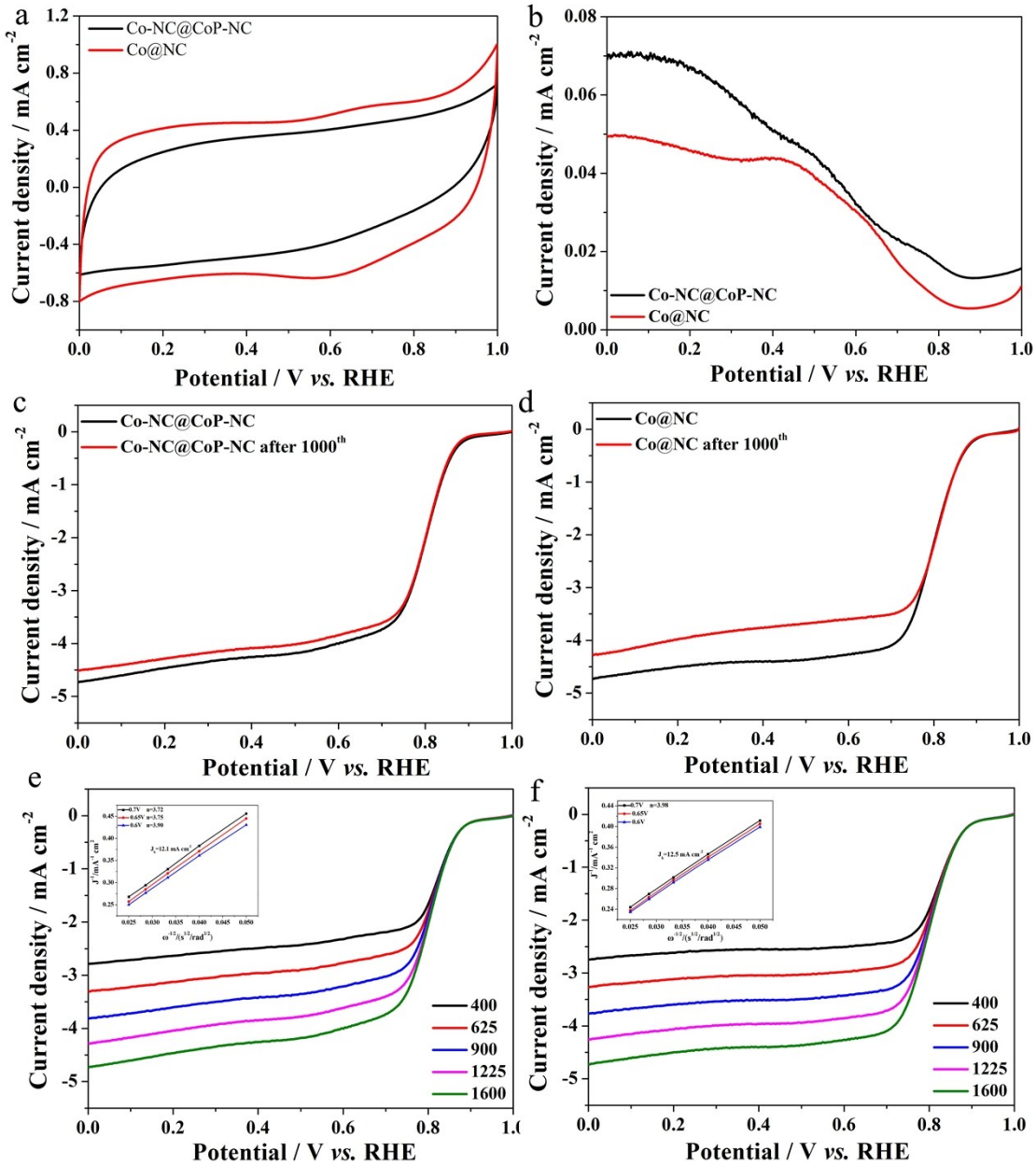

Fig. S14 (a) The cyclic voltammograms (CVs) on Co-NC@CoP-NC and Co@NC in N_2-saturated in 0.1 M KOH. (b) Faradaic ring current of Co-NC@CoP-NC and Co@NC. (c) LSV of Co-NC@CoP-NC and after 1000 cycles. (d) LSV of Co@NC and after 1000cycles. (e) and (f) Koutecky–Levich (KL) plots and J_k was obtained from the LSVs at various rotating speeds on Co-NC@CoP-NC and Co@NC.

With the tested disc and ring currents, we can calculate the electron transfer number (n) of ORR according to the following equation:

$$n = \frac{4 j_D}{j_D + \frac{j_R}{N}}$$

In this equation, j_D is the faradic disc current, j_R is the faradic ring current (Fig. S8b), and N is the collection efficiency (0.37) of the ring electrode.

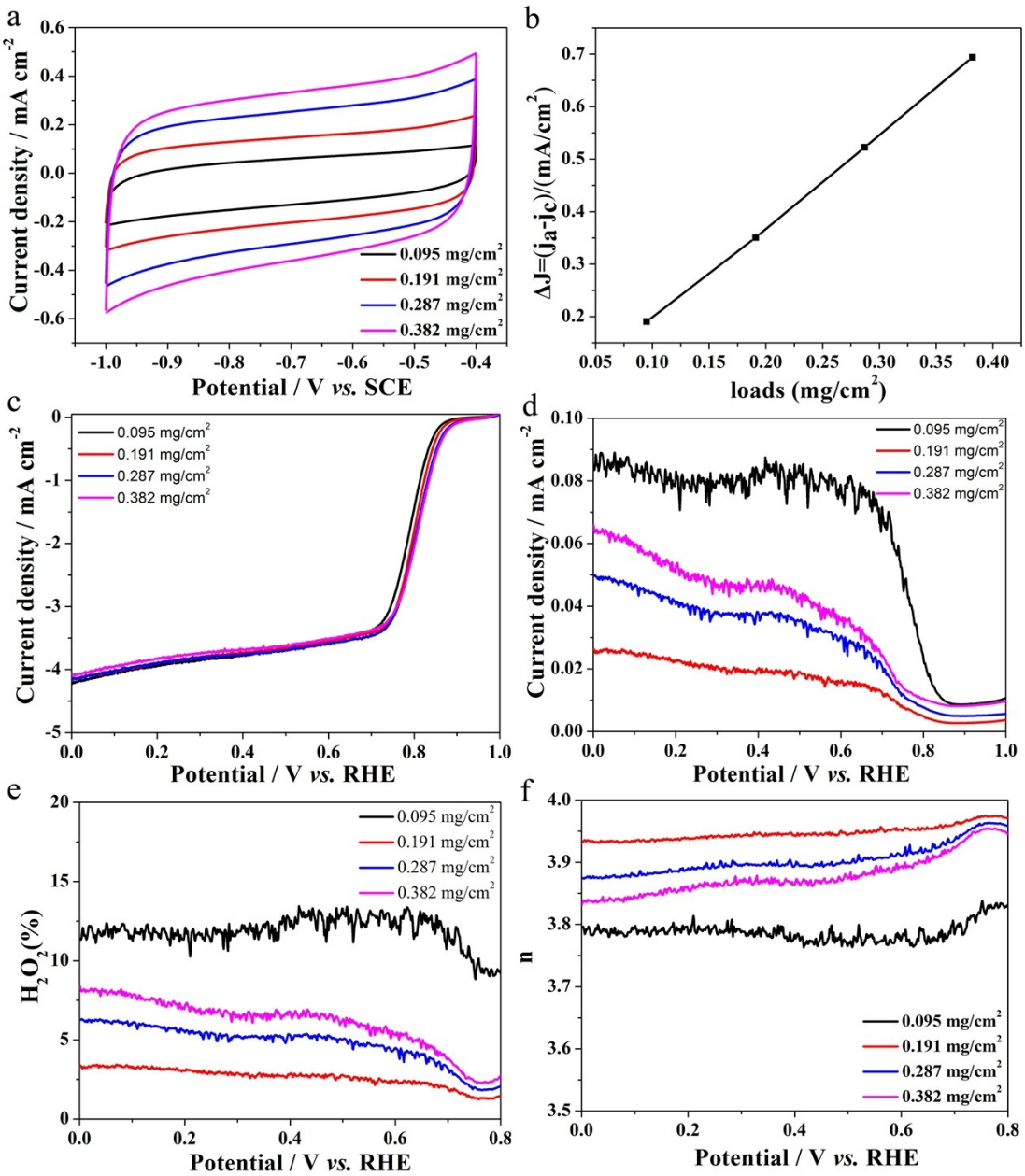

Fig S15 (a) CV curves of Co-NC@CoP-NC with different loadings in N_2-saturated 0.1 M KOH. (b) Linear relationship of Co-NC@CoP-NC with different loadings. (c) Oxygen reduction current on the disk and (d) ring current divided by collection efficiency. (e) The obtained peroxide yield of Co-NC@CoP-NC with different loadings. (f) The electron transfer number of Co-NC@CoP-NC with different loadings.

Table S3 Comparison of electrocatalytic OER and ORR activity of recently reported nonprecious eectrocatalysts

Catalyst	Precursor	Substrate*	Mass loading (mg cm^{-2})	OER performance			ORR performance			Reference
				Electrolyte	Onset potential (V vs. RHE)	Potential @10 mA cm^{-2} (V vs. RHE)	Electrolyte	Onset potential (V vs. RHE)	Half-wave potential (V vs. RHE)	
Co-NC@CoP-NC	ZIF-67	GCE	0.28	0.1 M KOH	1.47	1.56	0.1 M KOH	0.88	0.78	This work
Co@NC	ZIF-67	GCE	0.28	0.1 M KOH	1.56	1.71	0.1 M KOH	0.90	0.78	This work
RuO_2		GCE	0.28	0.1 M KOH	1.43	1.61	0.1 M KOH			This work
Pt		GCE	0.28	0.1 M KOH	1.60	1.75	0.1 M KOH	0.94		This work
NCNTFs	ZIF-67	GCE	0.20	0.1 M KOH	1.47	1.60	0.1 M KOH	0.97	0.87	S1
Fe/Fe_3C@NGL-NCNT	MIL-101(Fe)	GCE	0.16	0.1 M KOH		2.05	0.1 M KOH	1.01		S2
Co-CoO-Z9-800-250	ZIF-9	GCE	0.25	0.1 M KOH		~1.75	0.1 M KOH	0.92		S3
Co_xS_y@C-1000	ZIF-67	GCE	0.14	0.1 M KOH		1.71	0.1 M KOH	0.93		S4
Co@Co_3O_4/NC-1	ZIF-67	GCE	0.21	0.1 M KOH		1.64	0.1 M KOH	0.93	0.74	S5
$Co_{25}Zn_{75}$–C1100-10h	Co-Zn-ZIF	GCE	0.28	0.1 M KOH	~1.57	~1.70	0.1 M KOH	0(Ag/AgCl)	0.45	S6
N/Co-d-PCP//NRGO	ZIF-67	GCE	0.71	0.1 M KOH		1.66	0.1 M KOH	0.93	0.87	S7
Co_3O_4@C-MWCNT	ZIF-67	GCE	0.33	1.0 M KOH	1.50	1.55	0.1 M KOH	0.89	0.81	S8
Co-CNT/PC	ZIF-67	NF	1.00	0.1 M KOH	~1.42	1.55	0.1 M KOH	0.92		S9
$LaNiO_3$ Perovskites		GCE		0.1 M KOH	~1.52	~1.59	0.1 M KOH	0.90		S10
$CoFe_2O_4$/RC-400		GCE	0.32	0.1 M KOH	1.37	1.56	0.1 M KOH	0.87		S11
Co_3O_4/CNW		GCE	0.13	0.1 M KOH	~1.50	~1.57	0.1 M KOH	0.85		S12
CoO/N-doped graphene		GCE	0.70	1.0 M KOH	1.30	1.57	1.0 M KOH	0.94	0.81	S13
$Co_{0.5}Fe_{0.5}S$@N-MC		GCE	0.88	1.0 M KOH	1.57	~1.65	0.1 M KOH	~0.88	~0.80	S14

Co_3O_4/N-d-graphene		NF	1.00	1.0 M KOH	1.30	1.57	0.1 M KOH	0.90	0.83	S15
Fe/C/N		GCE	0.20	0.1 M KOH		1.59	0.1 M KOH		0.83	S16
NPMC-1000		GCE	0.15	0.1 M KOH	1.30	>1.90	0.1 M KOH	0.94	0.85	S17
CNNT-ACN		GCE	0.46	0.1 M KOH		1.68	0.1 M KOH	0.93	0.74	S18
N,P-GCNS		GCE	0.14	0.1 M KOH	1.32	1.57	0.1 M KOH	1.01		S19
PCN–CFP		CFP	0.20	0.1 M KOH	1.53	1.63	0.1 M KOH	0.94	0.67	S20
CoP nanoparticle		GCE	0.40	0.1 M KOH	1.45	1.57				S21
Co-P film		CF		1.0 M KOH	1.50	1.58				S22
CoP hollow polyhedron	ZIF-67	GCE	0.10	1.0 M KOH	1.53	1.63				S23
CoP/NC	ZIF-67	GCE	0.28	1.0 M KOH	~1.50	1.58				S24
CoP/rGO-400	ZIF-67	GCE	0.28	1.0 M KOH	~1.50	1.57				S25
ZIF/rGO-700-AL	ZIF-67	GCE	0.41				0.1 M KOH	0.93		S26
Co-N-C	$Zn_{0.8}Co_{0.2}(MeIM)_2$	GCE	0.28				0.1 M KOH	~0.96	0.87	S27
CNCo-40	$Zn_{0.2}Co_{0.8}(MeIM)_2$	GCE	0.10				0.1 M KOH	0.89	0.82	S28
ZIF-67-900-	ZIF-67	GCE	0.36				0.1 M KOH	0.91	0.85	S29

* NF: nickel foam; GCE: glassy carbon electrode; CFP: carbon-fiber paper; CF: copper foil

S1. B. Y. Xia, Y. Yan, N. Li, H. B. Wu, X. W. Lou and X. Wang, *Nature Energy*, 2016, 1, 15006.

S2. J.-S. Li, S.-L. Li, Y.-J. Tang, M. Han, Z.-H. Dai, J.-C. Bao and Y.-Q. Lan, *Chem. Commun.*, 2015, 51, 2710-2713.

S3. W. Chaikittisilp, N. L. Torad, C. L. Li, M. Imura, N. Suzuki, S. Ishihara, K. Ariga and Y. Yamauchi, *Chem.- Eur. J.*, 2014, 20, 4217-4221.

S4. B. Chen, R. Li, G. Ma, X. Gou, Y. Zhu and Y. Xia, *Nanoscale*, 2015, 7, 20674-20684.

S5. A. Aijaz, J. Masa, C. Rosler, W. Xia, P. Weide, A. J. Botz, R. A. Fischer, W. Schuhmann and M. Muhler, *Angew. Chem. Int. Ed.*, 2016, 55, 4087-4091.

S6. G. Srinivas, T. Zhao, S. A. Shevlin and Z. X. Guo, *Energy Environ. Sci.*, 2016, 9, 1661-1667.

S7. Y. Hou, Z. Wen, S. Cui, S. Ci, S. Mao and J. Chen, *Adv. Funct. Mater.*, 2015, 25, 872-882.

S8. X. Z. Li, Y. Y. Fang, X. Q. Lin, M. Tian, X. C. An, Y. Fu, R. Li, J. Jin and J. T. Ma, *J. Mater. Chem. A*, 2015, 3, 17392-17402.

S9. S. Dou, X. Li, L. Tao, J. Huo, and S. Wang, *Chem. Commun.*, 2016, 52,9727-9730.

S10. J. R. Petrie, V. R. Cooper, J. W. Freeland, T. L. Meyer, Z. Y. Zhang, D. A. Lutterman and H. N. Lee, *J. Am. Chem. Soc.*, 2016, 138, 2488-2491.

S11. P. X. Li, R. G. Ma, Y. Zhou, Y. F. Chen, Z. Z. Zhou, G. H. Liu, Q. Liu, G. H. Peng, Z. H. Liang and J. Wang, *J. Mater. Chem. A*, 2015, 3, 15598-15606.

S12. S. Y. Liu, L. J. Li, H. S. Ahnb and A. Manthiram, *J. Mater. Chem. A*, 2015, 3, 11615-11623.

S13. S. Mao, Z. Wen, T. Huang, Y. Hou and J. Chen, *Energy Environ. Sci.*, 2014, 7, 609-616.

S14. M. X. Shen, C. P. Ruan, Y. Chen, C. H. Jiang, K. L. Ai and L. H. Lu, *Acs Appl. Mater. Interfaces*, 2015, 7, 1207-1218.

S15. Y. Liang, Y. Li, H. Wang, J. Zhou, J. Wang, T. Regier and H. Dai, *Nat. Mater.*, 2011, 10, 780-786.

S16. Y. Zhao, K. Kamiya, K. Hashimoto and S. Nakanishi, *J. Phys. Chem. C*, 2015, 119, 2583-2588.

S17. J. T. Zhang, Z. H. Zhao, Z. H. Xia and L. M. Dai, *Nat. Nanotechnol.*, 2015, 10, 444-452.

S18. R. M. Yadav, J. J. Wu, R. Kochandra, L. L. Ma, C. S. Tiwary, L. H. Ge, G. L. Ye, R. Vajtai, J. Lou and P. M. Ajayan, *Acs Appl. Mater. Interfaces*, 2015, 7, 11991-12000.

S19. R. Li, Z. D. Wei and X. L. Gou, *Acs Catalysis,* 2015, 5, 4133-4142.

S20. T. Y. Ma, J. Ran, S. Dai, M. Jaroniec and S. Z. Qiao, *Angew. Chem. Int. Ed.*, 2015, 54, 4646-4650.

S21. J. Ryu, N. Jung, J. H. Jang, H. J. Kim and S. J. Yoo, *Acs Catal.*, 2015, 5, 4066-4074.

S22. N. Jiang, B. You, M. Sheng and Y. Sun, *Angew. Chem. Int. Ed.*, 2015, 54, 6251-6254.

S23. M. Liu and J. Li, *Acs Appl. Mater. Interfaces*, 2015, 8, 2158-2165.

S24. B. You, N. Jiang, M. Sheng, S. Gul, J. Yano and Y. Sun, *Chem. Mater.*, 2015, 27, 7636-7642.

S25. L. Jiao, Y.-X. Zhou and H.-L. Jiang, *Chem. Sci.*, 2016, 7, 1690-1695.

S26. J. Wei, Y. Hu, Z. Wu, Y. Liang, S. Leong, B. Kong, X. Zhang, D. Zhao, G. P. Simon and H. Wang, *J. Mater. Chem. A*, 2015, 3, 16867-16873.

S27. B. You, N. Jiang, M. Sheng, W. S. Drisdell, J. Yano and Y. Sun, *ACS Catal.*, 2015, 5, 7068-7076.

S28. Y.-Z. Chen, C. Wang, Z.-Y. Wu, Y. Xiong, Q. Xu, S.-H. Yu and H.-L. Jiang, *Adv. Mater.*, 2015, 27, 5010-5016.

S29. X. Wang, J. Zhou, H. Fu, W. Li, X. Fan, G. Xin, J. Zheng and X. Li, *J. Mater. Chem. A*, 2014, 2, 14064-14070.